Photodissociation spectroscopy of (benzene–toluene)$^+$. Charge delocalization in the hetero-dimer ion

Kazuhiko Ohashi [a], Youko Nakane [a], Yoshiya Inokuchi [b], Yasuhiro Nakai [a], Nobuyuki Nishi [b,*]

[a] *Department of Chemistry, Faculty of Science, Kyushu University, Hakozaki, Fukuoka 812-8581, Japan*

[b] *Institute for Molecular Science, Myodaiji, Okazaki 444-8585, Japan*

Abstract

The electronic spectrum of the benzene–toluene hetero-dimer ion is measured in the 380–1400 nm region. The spectrum shows intense bands around 1175 and 670 nm and a weaker band around 920 nm, which correspond to charge resonance (CR) bands of homo-dimer ions. The observation indicates that the positive charge stays on the benzene part in some probability, although the ionization potential of benzene is 0.4162 eV higher than that of toluene. A local excitation band (LE) is observed around 420 nm, where a $\pi \leftarrow \pi$ transition is locally excited in the charged benzene or toluene molecule. On the basis of the position of the CR-like bands as well as the intensity of the LE band relative to that of homo-dimer ions, the probability of finding the charge on the benzene molecule is analyzed to be approximately 36 %.

* To whom correspondence should be addressed.

1. Introduction

Spectroscopic studies of dimer ions have provided insights into the nature of intermolecular interactions between the component molecules. In condensed phases, conventional absorption spectroscopy was applied to dimer ions of aromatic molecules [1–3]. Recently, we have measured electronic spectra of dimer ions of benzene [4–6] and naphthalene [7] by mass-selected photodissociation spectroscopy in the gas phase. Two types of absorption bands are commonly seen on the spectra in the region from the visible to near-infrared. One is a charge resonance (CR) band. In a dimer ion composed of molecules X and Y, namely $(XY)^+$, the attractive CR interaction provides the ground state described by the wave function: $\Psi_+ = \alpha\psi(X^+)\psi(Y) + \beta\psi(X)\psi(Y^+)$, where $\alpha^2 + \beta^2 = 1$. The repulsive interaction produces the excited state: $\Psi_- = \beta\psi(X^+)\psi(Y) - \alpha\psi(X)\psi(Y^+)$. The CR band arises from the transition between the two CR states, Ψ_+ and Ψ_-. The other type is a local excitation (LE) band. An electronic transition is locally excited in a monomer ion unit (X^+ or Y^+). For each homo-dimer ion (X = Y) studied so far [5–7], the CR band is much stronger than the LE band. The observation indicates that the positive charge is equally shared with the two component molecules as a result of strong CR interaction.

In a hetero-dimer ion comprised of dissimilar partners ($X \neq Y$), the charge may stay mainly on the molecule with lower ionization potential (IP). A limited number of absorption spectra were reported for hetero-dimer ions of aromatic molecules in condensed phases [8,9]. Meot-Ner and co-workers measured enthalpies of dissociation for a series of hetero-dimer ions by high-pressure mass spectrometry [10,11]. The enthalpies were found to decrease with increasing the difference in the IP's (ΔIP) of the component molecules. Neusser and co-workers determined the dissociation energies of several dimer ions from the ionization potentials of neutral dimers and the appearance potentials for the dissociation of dimer ions (breakdown measurement) [12–14]. The dissociation energies of hetero-dimer ions of benzene with other molecules were found to be smaller than that of the benzene homo-dimer ion. Both groups assigned the decreased dissociation energy in hetero-dimer ions to the reduced resonance interaction [10–14].

We plan to study hetero-dimer ions of benzene with a series of other aromatic molecules as a function of ΔIP. We have already published the results of the benzene–naphthalene hetero-dimer ion [15]. The photodissociation spectrum of (benzene–naphthalene)$^+$ shows three distinct bands in the 400–1200 nm region. The most intense band around 580 nm is an LE band of the (naphthalene)$^+$ chromophore. In addition to this band, we observe an LE band of the (benzene)$^+$ chromophore. The observation indicates that the positive charge stays on the benzene part in some probability despite a large ΔIP of 1.10 eV. The spectrum also shows an intermolecular charge transfer (CT) band around 920 nm. On the basis of the position of the CT band as well as the intensity of the LE band relative to that of $(benzene)_2^+$, the probability of finding the charge on the benzene molecule is analyzed to be approximately 9 %. Similar studies on other hetero-dimer ions provide additional important information on CR and CT interactions. In this article, we report the results of the benzene–toluene hetero-dimer ion (abbreviated as BT$^+$ hereafter). The IP's of benzene (B) and toluene (T) are determined to be 9.243842 [16] and 8.8276 eV [17], respectively, resulting in ΔIP of 0.4162 eV. We choose this system for the purpose of bridging the gap between B_2^+ (ΔIP = 0) and (benzene–naphthalene)$^+$ (ΔIP = 1.10 eV).

2. Experimental

We use two different sets of experimental apparatus. Each apparatus consists of a cluster-beam source and a tandem mass spectrometer with a quadrupole ion trap. Neutral clusters are formed by expanding a mixture of benzene and toluene with argon gas through a pulsed valve. The clusters are subsequently ionized by either resonant 2-photon ionization (R2PI) or laser-induced plasma technique [18]. The first mass filter isolates specific cluster ions for photoexcitation. The excited parent ions undergo fragmentation. The second mass filter analyzes mass number of photofragment ions. Photodissociation spectra are obtained from yields of the fragment ions as functions of wavelengths of the excitation laser.

Photodissociation spectra in the LE band region (380–480 nm) are recorded by using an apparatus with an octopole ion guide and two quadrupole mass filters [7,15]. Cluster ions are prepared in laser-induced plasma. The parent ion of interest is isolated through the first

quadrupole mass filter. After deflection by an ion bender, the ion beam is introduced into the octopole ion guide. A dissociation laser beam merges with the ion beam in the ion guide. The resulting photofragment ions are analyzed by the second quadrupole filter.

Overall photodissociation spectra are measured by using an apparatus with a reflectron-type time-of-flight (TOF) mass spectrometer [4,6]. Cluster ions are formed by R2PI of neutral clusters. The first TOF instrument selects the parent ion of interest. A dissociation laser irradiates a packet of the selected ion in the acceleration region of the mass spectrometer. Analysis of the photofragment ions is performed through an ion reflector. For measuring photodissociation cross sections of T_2^+ and BT^+ relative to those of B_2^+, the dissociation laser beam is adjusted to irradiate the packets of these three ions simultaneously. The relative cross sections are obtained from the measurement of the depletion efficiency of the parent ions [19].

The TOF mass spectrometer is also used for hole-burning experiments on mass-selected BT^+. Details of the experimental method have been reported previously [20]. Briefly, a hole-burning laser (λ_h) irradiates the packet of BT^+ in the acceleration region, yielding a permanent reduction of the number of the ions in the packet. Subsequently, the ion packet is crossed by a probe laser beam (λ_p) in the field-free drift region. When the hole-burning laser depopulates the species selected by the probe laser, the depopulation is seen as a depletion of the signal monitored by the probe laser.

3. Results and discussion

3.1. Photodissociation spectra of homo-dimer ions

Information on the electronic structures of the homo-dimer ions B_2^+ and T_2^+ is indispensable for interpreting the spectrum of BT^+. The overall photodissociation spectrum of T_2^+ is measured in this work by using the TOF mass spectrometer. The spectrum of B_2^+ was already reported in our previous publications [4–6]. These spectra are shown in Fig. 1. The 430 and 580 nm bands of B_2^+ are the LE bands of $\pi_{2,3}(e_{1g}) \leftarrow \pi_1(a_{2u})$ and $\pi_{2,3}(e_{1g}) \leftarrow \sigma(e_{2g})$ transitions, respectively [4,6]. The 920 and 1160 nm bands of B_2^+ are the CR bands [5,6,20]. The spectrum of T_2^+ exhibits two distinct maxima around 440 and 980 nm. Several

groups reported the optical absorption spectrum [1,21] and the photodissociation spectrum [22,23] of T^+. The latter spectrum shows a $\pi_3(b_1) \leftarrow \pi_1(a_1)$ transition around 420 nm. Therefore, the 440 nm band of T_2^+ is attributed to the LE band of the $\pi_3(b_1) \leftarrow \pi_1(a_1)$ transition. The LE band of a $\pi_3(b_1) \leftarrow \sigma(a_1)$ transition is expected around 500 nm, according to the photoelectron spectrum of toluene [24]. However, the corresponding feature is not seen in the photodissociation spectrum of T_2^+. The 980 nm band of T_2^+ is assigned to the CR band. We can determine the degree of the resonance interaction from the position of the CR band, as far as configuration interactions of the CR states with other electronically excited states are negligibly small [6]. The effect of methyl substitution in producing the red shift from B_2^+ (920 nm) to T_2^+ (980 nm) was explained as a steric effect [1]. We compared the CR transition energy of B_2^+ and T_2^+ measured by our group and the binding energy reported by Neusser and co-workers [12]. For each homo-dimer ion, the CR transition energy was found to be just twice as much as the binding energy [6]. The result suggests that the dominant contribution to the binding energy of B_2^+ and T_2^+ is from the resonance interaction, in accordance with the conclusion by Neusser and co-workers.

3.2. Dissociation channels of BT^+

Upon photoexcitation in the region from the visible to near-infrared, BT^+ may dissociate in two different ways as follows:

$$BT^+ + h\nu \rightarrow B^+ + T, \quad (1a)$$

$$BT^+ + h\nu \rightarrow B + T^+. \quad (1b)$$

At all wavelengths studied here, the dissociation of BT^+ is found to yield $B + T^+$ predominantly. The behavior is similar to that of (benzene–naphthalene)$^+$ [15]. In both cases, the component molecule with lower IP always appears as the fragment ion, regardless of the nature of the photoexcited states. Therefore, monitoring the yield of T^+ alone is enough to obtain the photodissociation spectrum of BT^+.

3.3. Photodissociation spectrum of BT^+

Figure 2 shows the photodissociation spectrum of BT^+. Four distinct maxima are seen around 420, 670, 920 and 1175 nm. The 420 nm band can be attributed to an LE band. Three other bands must arise from intermolecular interactions in the hetero-dimer ion, because there are no LE bands in the corresponding region of the spectra of B_2^+ and T_2^+. One may suppose that conformational isomers of BT^+ are responsible for the appearance of these bands. We perform hole-burning experiments to address the question of existence of isomers of BT^+.

3.4. Hole-burning experiments

Figure 3 exhibits arrival-time spectra of fragment ions recorded in the hole-burning experiments on BT^+. The top two spectra are obtained with the hole-burning laser at 670 nm and the probe laser at 1175 nm. Only the signal of T^+ due to the probe laser, namely the probe-laser signal, appears at 36.8 μs on spectrum (a) recorded with the probe laser alone. Introduction of the hole-burning laser yields spectrum (b). Spectrum (b) displays a decrease in the probe-laser signal with respect to the corresponding signal on spectrum (a). The result indicates that both lasers excite the same species, otherwise the intensity of the probe-laser signal would be independent of the hole-burning laser. Because of the secondary acceleration [20], the signal of T^+ due to the hole-burning laser shifts to a shorter arrival time and appears at 33.8 μs. The bottom two spectra are obtained with the hole-burning laser at 670 nm and the probe laser at 920 nm. Spectrum (c) is recorded with the probe laser alone. Spectrum (d) also demonstrates that the intensity of the probe-laser signal is reduced by the introduction of the hole-burning laser. We therefore conclude that *the three distinct transitions of a single BT^+* are responsible for the bands at 670, 920 and 1175 nm. The LE band around 420 nm is also due to the same conformation of BT^+.

3.5. Local excitation band

Figure 4 represents an expanded view of the photodissociation spectra of B_2^+, BT^+ and T_2^+ in the LE band region. Our previous study of (benzene–naphthalene)$^+$ revealed that the positive charge stays on the benzene part with the probability of 9 %, although the IP of benzene is by 1.10 eV higher than that of naphthalene [15]. In BT^+, the charge is expected to

reside on the benzene part with a probability higher than that in (benzene–naphthalene)$^+$, because ΔIP between B and T is smaller than ΔIP between benzene and naphthalene. Therefore, the LE band of BT$^+$ is composed of the contribution not only from the T$^+$ part but also from the B$^+$ part. However, we cannot decompose the spectrum of BT$^+$ into two components, because the LE bands of B_2^+ (due to the B$^+$ chromophore) and T_2^+ (due to the T$^+$ chromophore) just overlap with each other. Then, we direct our attention to the integrated intensities of these bands. The area under the absorption curve for B_2^+, $I(B_2^+)$, is proportional to the oscillator strength of the $\pi_{2,3} \leftarrow \pi_1$ transition of the B$^+$ chromophore. Similarly, the area under the T_2^+ curve, $I(T_2^+)$, is proportional to the oscillator strength of the $\pi_3 \leftarrow \pi_1$ transition of the T$^+$ chromophore. Here, we assume that the oscillator strengths of the transitions are independent of the neutral partner, *i.e.*, the effect on the B$^+$ chromophore of B in (B$^+$···B) is the same as that of T in (B$^+$···T) and the influence on the T$^+$ chromophore of T in (T···T$^+$) is the same as that of B in (B···T$^+$). In such a case, the area under the BT$^+$ curve is given by

$$I(BT^+) = p\, I(B_2^+) + (1-p)\, I(T_2^+), \qquad (2)$$

where p is the probability of finding the charge on the B part in BT$^+$. From the spectra shown in Fig. 4, we obtain the following ratios; $I(B_2^+):I(BT^+):I(T_2^+) = 1:1.2:1.3$. The value of p is determined to be 0.33 according to Eq. (2). This is an approximate estimation of the probability. However, this value agrees with a more reliable estimation derived in the next section.

3.6. Near-resonance interactions

Intermolecular interactions must be responsible for the absorption bands at 670, 920 and 1175 nm. Figure 5 depicts an energy level diagram for analyzing near-resonance interactions in BT$^+$. The B$^+$ + T dissociation limit is located above the B + T$^+$ limit by ΔIP (0.4162 eV). The dissociation energy of BT$^+$ into B + T$^+$ was determined to be $D_0 = 0.53$ eV [12]. This means that an attractive interaction lowers the ground state of BT$^+$ by 0.53 eV from the B + T$^+$ limit. In our previous study, we observed that the CR transition energy of B_2^+ is just twice as much as the binding energy [6]. The splitting between the two CR states of B_2^+ is symmetric about the energy of the separated B$^+$ and B. If we assume that near-resonance interactions in BT$^+$

raise and lower the energies by the same amount from those of the separated molecules, the excited state of BT^+ lies 0.53 eV above the $B^+ + T$ limit as a result of repulsive interaction. If the excited state is really located at this position, a CR-like band with the transition energy of $\Delta E = 2D_0 + \Delta IP$ would appear around 840 nm. However, any position of the observed bands is not coincident with the expected one. It is necessary to take into account the following details. First, the lowest excited state of the toluene ion (T^{+*}) lies approximately 0.53 eV above the ground state, according to the photoelectron spectrum [24]. The $B + T^{+*}$ dissociation limit and the $B^+ + T$ limit are located within 0.11 eV. Therefore, the CR excited state of BT^+ correlating to the $B^+ + T$ limit may interact with an LE state correlating to the $B + T^{+*}$ limit. Second, the ground state of the benzene ion is doubly degenerated, because the highest occupied molecular orbitals of benzene (π_2(B) and π_3(B)) are of e_{1g} symmetry. The π_3 orbital of T, π_3(T), has the same character as π_3(B); π_2(T) has the same character as π_2(B). The interaction between two orbitals of the same character is expected to be stronger than that between two orbitals of different character. As indicated in Fig. 5, two excited states are formed as a result of attractive and repulsive interactions of the CR excited state with the LE state correlating to the $B + T^{+*}$ limit. Each of the two states further splits into two levels due to the lift of the degeneracy of π_2(B) and π_3(B). The three bands observed at 670, 920 and 1175 nm can be assigned to the transitions from the ground state to three of the resulting four excites states. The fourth band due to the transition to the rest of the excited states is expected to appear around 800 nm. Although the corresponding maximum is not clearly seen on the spectrum, the shape of the 670 and 920 nm bands is asymmetric and the cross sections are appreciable in the region between the two bands.

Now, we estimate the probability distribution of the charge in BT^+. We applied a simple perturbation theory to (benzene–naphthalene)$^+$ [15]. We took account of only near-resonance interactions and assumed that the interactions raise and lower the unperturbed energies of the separated molecules by the same amount. In order to treat BT^+ in a similar way, we hypothesize an excited state by 0.53 eV (= D_0) above the $B^+ + T$ limit. Magnitude of the shift of the excited state may not be equal to that of the ground state, since the charge–dipole interaction may lower the CR states especially correlating to the $B^+ + T$ limit. Nevertheless, the

location of the hypothetical state is consistent with the fact that the transition energy from the ground state to the hypothetical state (ΔE = 1.48 eV) is in good agreement with the average (1.45 eV) of the transition energies observed for the 1175 and 670 nm bands (Fig. 5). The wave function of BT^+ can be written as

$$\Psi = \alpha\psi(B^+)\psi(T) + \beta\psi(B)\psi(T^+), \quad (3)$$

where α^2 and β^2 stand for the probabilities of finding the charge on B and T, respectively. The perturbed energies are given by

$$E_+ = (1/2)(H_{BB} + H_{TT}) - (1/2)[(H_{BB} - H_{TT})^2 + 4H_{BT}^2]^{1/2}, \quad (4a)$$

$$E_- = (1/2)(H_{BB} + H_{TT}) + (1/2)[(H_{BB} - H_{TT})^2 + 4H_{BT}^2]^{1/2}, \quad (4b)$$

for the ground and excited states, respectively, where $H_{BB} = \langle\psi(B^+)\psi(T)\,|\,H\,|\,\psi(B^+)\psi(T)\rangle$, $H_{TT} = \langle\psi(B)\psi(T^+)\,|\,H\,|\,\psi(B)\psi(T^+)\rangle$ and $H_{BT} = \langle\psi(B^+)\psi(T)\,|\,H\,|\,\psi(B)\psi(T^+)\rangle$. Then the transition energy between the two states is given by

$$\Delta E = E_- - E_+ = [(H_{BB} - H_{TT})^2 + 4H_{BT}^2]^{1/2}. \quad (5)$$

Substitution of 1.45 eV for ΔE and 0.4162 eV (ΔIP) for $(H_{BB} - H_{TT})$ in Eq. (5) results in H_{BT} = 0.69 eV. Finally, we obtain the following wave functions

$$\Psi_+ = (0.36)^{1/2}\psi(B^+)\psi(T) + (0.64)^{1/2}\psi(B)\psi(T^+), \quad (6a)$$

$$\Psi_- = (0.64)^{1/2}\psi(B^+)\psi(T) - (0.36)^{1/2}\psi(B)\psi(T^+), \quad (6b)$$

for the ground and excited states, respectively. In the ground state, the probability of finding the charge on the T part is 0.64 and that on the B part is 0.36. This value is in good agreement with that obtained from the crude analysis of the integrated intensities of the LE bands in the previous section.

3.7. Charge delocalization

Meot-Ner and co-workers examined relation between enthalpy of dissociation (ΔH°_D) and ΔIP for B^+ with a series of neutral molecules [11]. ΔH°_D was observed to decrease monotonically with increasing ΔIP from the largest value of 0.74 eV for B_2^+ (ΔIP = 0) to 0.46 eV for (benzene–1,3,5-trimethylbenzene)$^+$ with ΔIP = 0.83 eV. The results suggest that

resonance interactions between the two components decrease with increasing ΔIP, because the component with lower IP increasingly retains the positive charge.

With the treatment described in the previous section, we can evaluate the degree of the charge delocalization in hetero-dimer ions. Figure 6 indicates the probability of finding the charge on the benzene molecule as a function of ΔIP for B_2^+, BT^+, (benzene–*p*-xylene)$^+$ and (benzene–naphthalene)$^+$. The probability decreases almost linearly with increasing ΔIP, at least up to ΔIP = 1.10 eV. The tendency is totally consistent with the relation between the binding energy and ΔIP.

4. Conclusion

The photodissociation spectrum of BT^+ exhibits four bands at 420, 670, 920 and 1175 nm. The 420 nm band is assigned to the LE band, in which both B^+ and T^+ have a chance to act as the chromophore. The 670, 920 and 1175 nm bands are attributed to the CR-like bands, which arise from near-resonance interactions between the component molecules. The intensity of the CR-like bands is much larger than that of the LE band. The transition energy of the CR-like bands is more than three times as large as ΔIP. On the basis of the transition energy, the probability of finding the charge on the benzene molecule is analyzed to be approximately 36 %. These results are in contrast to those of (benzene–naphthalene)$^+$. The near-infrared band of (benzene–naphthalene)$^+$ is weaker than the LE band, and the transition energy is only 1.23 times larger than ΔIP. The probability of finding the charge on the benzene part is only 9 %. The near-infrared band of (benzene–naphthalene)$^+$ has a character of a charge transfer band rather than a charge resonance band. On the other hand, near-resonance interaction is still important in BT^+ with ΔIP = 0.4162 eV as well as the CR interactions in the homo-dimer ions.

Acknowledgement

We thank Messrs. T. Shibata and K. Adachi for their help in measuring the photodissociation spectrum of toluene dimer ion. This work was supported in part by a Grant-in-Aid for research program (07740465) from the Ministry of Education, Science, Sports and Culture of Japan.

References

[1] B. Badger and B. Brocklehurst, Trans. Faraday Soc. 65 (1969) 2582.

[2] A. Kira and M. Imamura, J. Phys. Chem. 83 (1979) 2267.

[3] T. Shida, Electronic absorption spectra of radical ions (Elsevier, Amsterdam, 1988) p. 12.

[4] K. Ohashi and N. Nishi, J. Chem. Phys. 95 (1991) 4002.

[5] K. Ohashi and N. Nishi, J. Phys. Chem. 96 (1992) 2931.

[6] K. Ohashi Y. Nakai, T. Shibata and N. Nishi, Laser Chem. 14 (1994) 3.

[7] Y. Inokuchi, K. Ohashi, M. Matsumoto and N. Nishi, J. Phys. Chem. 99 (1995) 3416.

[8] A. Kira, T. Nakamura and M. Imamura, Chem. Phys. Lett. 54 (1978) 582.

[9] A. Tsuchida, H. Takamura and M. Yamamoto Chem. Phys. Lett. 198 (1992) 193.

[10] M. Meot-Ner (Mautner), P. Hamlet, E. P. Hunter and F. H. Field, J. Am. Chem. Soc. 100 (1978) 5466.

[11] M. Meot-Ner (Mautner), J. Phys. Chem. 84 (1980) 2724.

[12] B. Ernstberger, H. Krause, A. Kiermeier and H. J. Neusser, J. Chem. Phys. 92 (1990) 5285.

[13] B. Ernstberger, H. Krause and H. J. Neusser, Z. Phys. D 20 (1991) 189.

[14] H. J. Neusser and H. Krause, Chem. Rev. 94 (1994) 1829.

[15] M. Matsumoto, Y. Inokuchi, K. Ohashi and N. Nishi, J. Phys. Chem. A 101 (1997) 4574.

[16] R. Neuhauser, K. Siglow and H. J. Neusser, J. Chem. Phys. 106 (1997) 896.

[17] K.-T. Lu, G. C. Eiden and J. C. Weisshaar, J. Phys. Chem. 96 (1992) 9742.

[18] S. M. Beck and J. H. Hecht, J. Chem. Phys. 96 (1992) 1975.

[19] K. Ohashi, Y. Inokuchi and N. Nishi, Chem. Phys. Letters 257 (1996) 137.

[20] K. Ohashi, Y. Inokuchi and N. Nishi, Chem. Phys. Letters 263 (1996) 167.

[21] T. Shida and W. H. Hamill, J. Chem. Phys. 44 (1966) 2375.

[22] P. P. Dymerski, E. Fu and R. C. Dunbar, J. Am. Chem. Soc. 96 (1974) 4109.

[23] R. C. Dunbar, Chem. Phys. Letters 32 (1975) 508.

[24] K. Kimura, S. Katsumata, Y. Achiba, T. Yamazaki and S. Iwata, Handbook of HeI photoelectron spectra of fundamental organic molecules (Japan Scientific Societies Press, Tokyo, 1981) p. 189.

Figure Captions

Fig. 1. Photodissociation spectra of benzene dimer ion (top) and toluene dimer ion (bottom). The B_2^+ spectrum has already been reported in our previous publications [4–6]. Error bars of the T_2^+ spectrum indicate one standard deviation of statistical uncertainties determined from repeated laser scans. Amplitude of the two spectra is scaled according to the following relative cross section; $\sigma(B_2^+):\sigma(T_2^+) = 1 : 1.0$ at 950 nm.

Fig. 2. Photodissociation spectrum of benzene–toluene hetero-dimer ion. Intensity of the fragment ion (T^+) is normalized according to the dissociation laser power, and the results are plotted against the wavelength of the laser. Error bars indicate one standard deviation of statistical uncertainties determined from repeated laser scans.

Fig. 3. Arrival-time spectra of the fragment ion produced in hole-burning experiments on BT^+. Spectrum (a) is recorded with the probe laser (1175 nm) alone. Spectrum (b) is recorded with the hole-burning laser (670 nm) followed by the probe laser (1175 nm). Spectrum (c) is recorded with the probe laser (920 nm) alone. Spectrum (d) is recorded with the hole-burning laser (670 nm) followed by the probe laser (920 nm). Signal of T^+ due to the hole-burning laser appears at 33.8 μs, while that due to the probe laser (probe-laser signal) is seen at 36.8 μs.

Fig. 4. Photodissociation spectra of B_2^+, BT^+ and T_2^+ in the LE band region. Amplitude of the three spectra is scaled according to the following relative cross sections; $\sigma(B_2^+):\sigma(BT^+):\sigma(T_2^+) = 1 : 1.5 : 1.0$ at 420 nm, $1 : 0.9 : 1.0$ at 430 nm and $1 : 1.2 : 1.6$ at 440 nm. The area under each curve is proportional to the oscillator strength of the transition, because the abscissa is the wavenumber of the dissociation laser.

Fig. 5. Energy level diagram for analyzing near-resonance interactions in BT^+. The $B^+ + T$ dissociation limit is located above the $B + T^+$ limit by ΔIP (0.4162 eV). The dissociation energy of BT^+ into $B + T^+$ is determined to be $D_0 = 0.53$ eV [12]. Near-resonance interaction between $B\cdots T^+$ and $B^+\cdots T$ locates the hypothetical excited state 0.53 eV ($= D_0$) above the $B^+ +$

T limit. Near-resonance interaction between $B^+\cdots T$ and $B\cdots T^{+*}$ (an LE state correlating to the $B + T^{+*}$ limit) makes the energy gap of the two excited states much wider. Each of the two states further splits into two levels due to the lift of the degeneracy (symmetry reduction) of π_2(B) and π_3(B). Although the energy difference (0.11 eV) between $B^+ + T$ and $B + T^{+*}$ is neglected, the transition energy from the ground state to the hypothetical excited state (ΔE = $2D_0 + \Delta IP$ = 1.48 eV) is in good agreement with the average (1.45 eV) of the transition energies observed for the 1175 and 670 nm bands. Main configurational changes of the SOMO electron upon the four types of excitations are also shown on the left side.

Fig. 6. Probability of finding the charge on the benzene molecule (α^2) as a function of ΔIP. The data are for B_2^+ (ΔIP = 0), BT^+ (ΔIP = 0.4162 eV), (benzene–*p*-xylene)$^+$ (ΔIP = 0.76 eV) and (benzene–naphthalene)$^+$ (ΔIP = 1.10 eV). We have found the absorption maximum of (benzene–*p*-xylene)$^+$ at 935 nm.

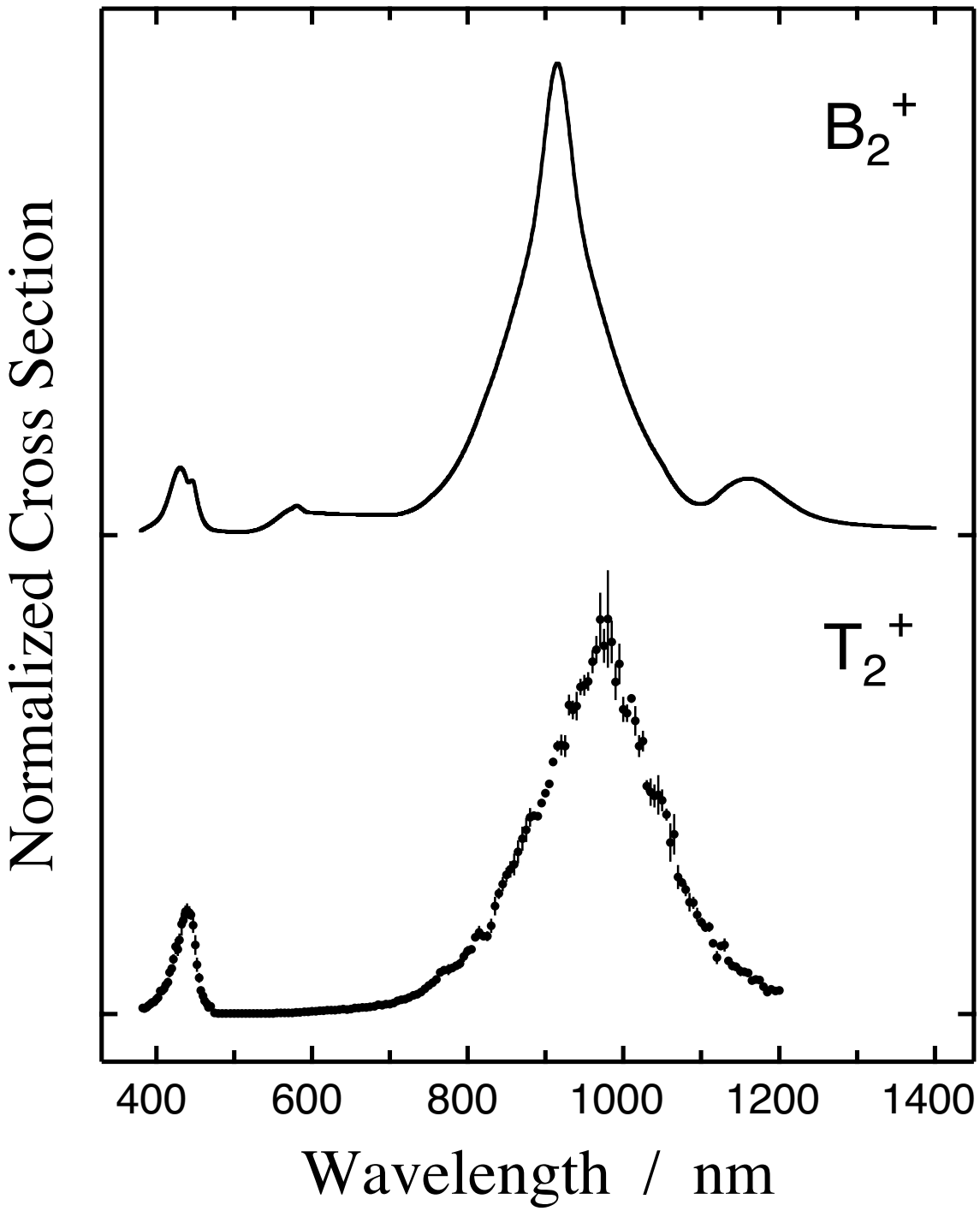

Fig. 1. Ohashi *et al*.

Fig. 2. Ohashi *et al.*

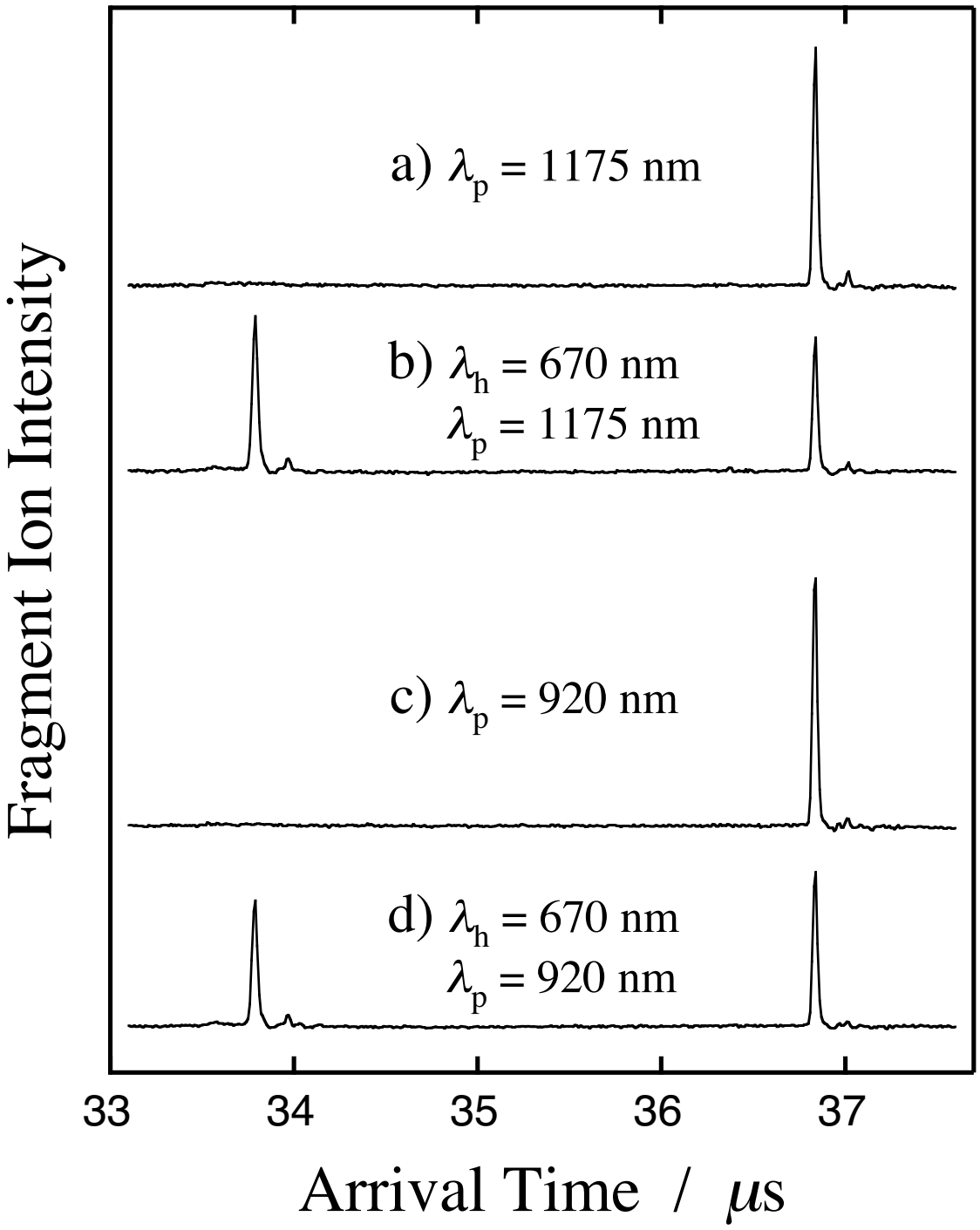

Fig. 3. Ohashi *et al*.

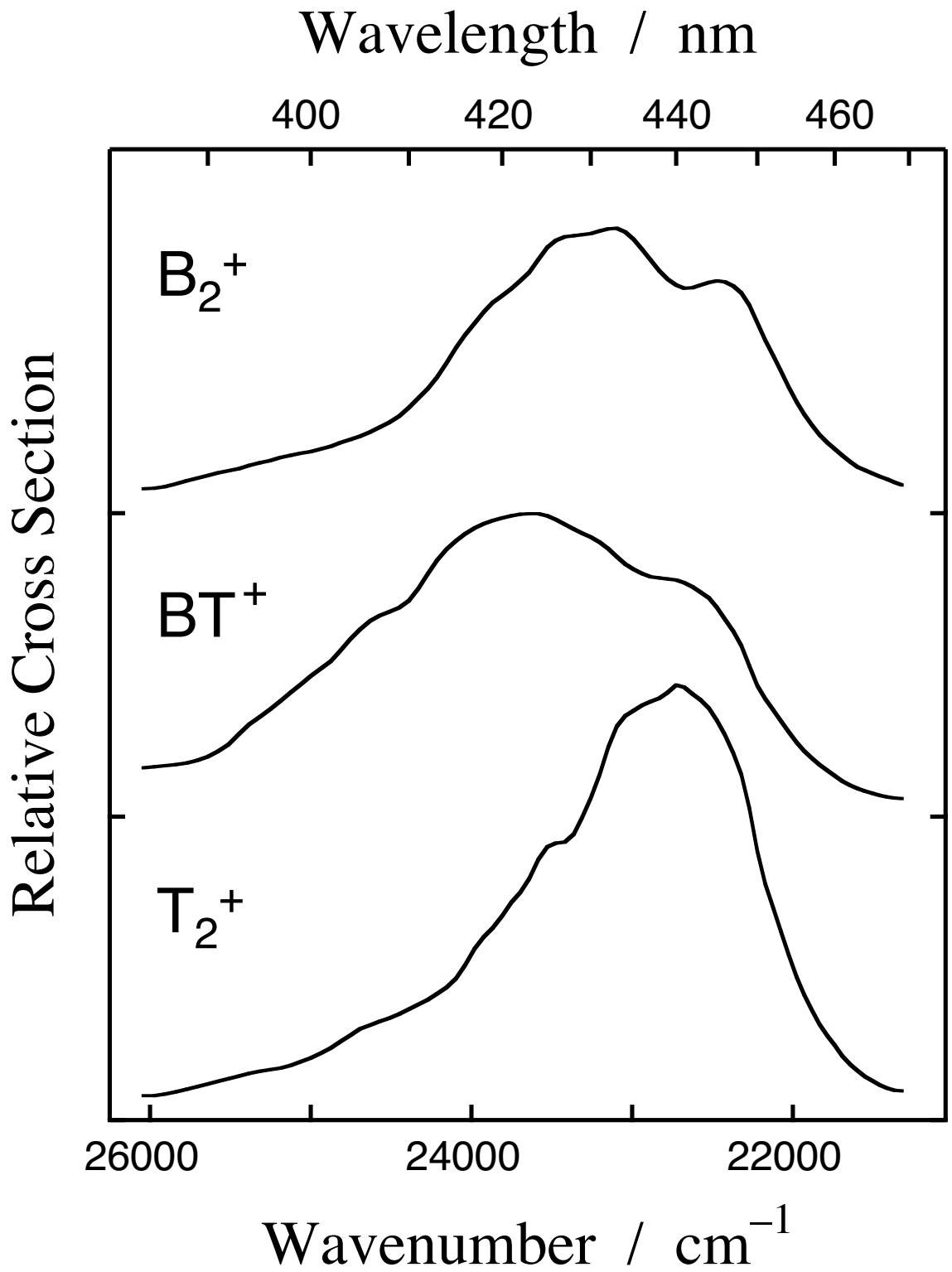

Fig. 4. Ohashi *et al*.

Fig. 5. Ohashi *et al.*

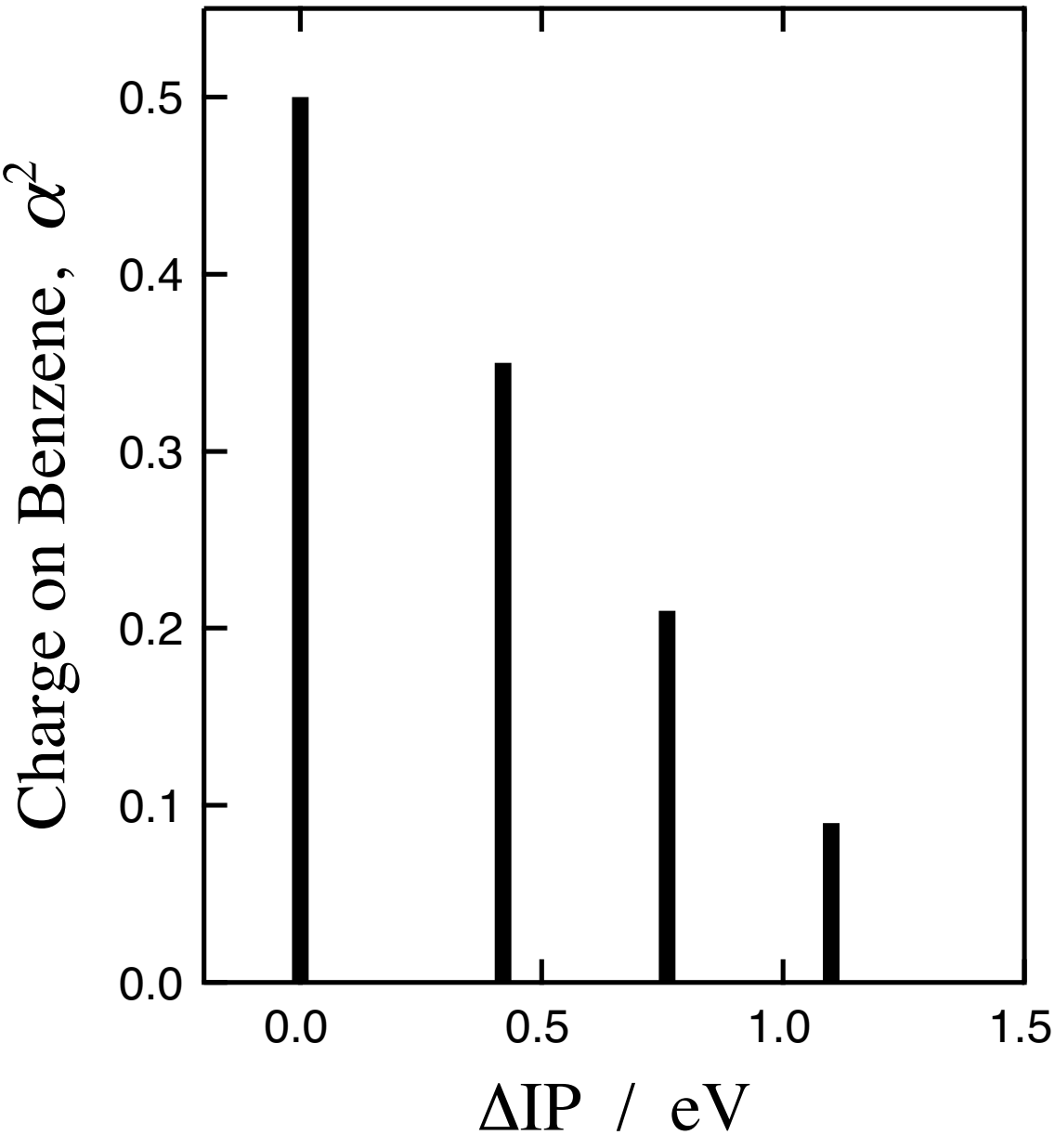

Fig. 6. Ohashi *et al*.